

Complex-Temperature Phase Diagrams of 1D Spin Models with Next-Nearest-Neighbor Couplings

Robert Shrock* and Shan-Ho Tsai**

Institute for Theoretical Physics
State University of New York
Stony Brook, N. Y. 11794-3840

Abstract

We study the dependence of complex-temperature phase diagrams on details of the Hamiltonian, focusing on the effect of non-nearest-neighbor spin-spin couplings. For this purpose, we consider a simple exactly solvable model, the 1D Ising model with nearest-neighbor (NN) and next-to-nearest-neighbor (NNN) couplings. We work out the exact phase diagrams for various values of J_{nnn}/J_{nn} and compare these with the case of pure nearest-neighbor (NN) couplings. We also give some similar results for the 1D Potts model with NN and NNN couplings.

PACS nos. 05.50.+q, 05.70.Fh, 64.60.-i, 64.60.Cn

*email: shrock@insti.physics.sunysb.edu

**email: tsai@insti.physics.sunysb.edu

1 Introduction

Yang and Lee pioneered a very interesting line of research in which one studies statistical mechanical models with the external magnetic field H generalized from real to complex values [1]. Since the free energy of a spin system $f = f(K, H)$ is a function of both the field H and the temperature T (or equivalently, $K = \beta J$, where $\beta = (k_B T)^{-1}$ and J is the spin-spin coupling), a related complexification is to generalize K from real to complex values. Both of these complexifications give one deeper insight into the properties of such models. Recently, there has been renewed interest in this subject for Ising models [2]-[10] and Potts models [11]-[13] (earlier references can be found in these papers). As the comparison of complex-temperature phase diagrams for the 2D (isotropic, nearest-neighbor) Ising model with spin $s \geq 1$ versus $s = 1/2$ in Refs. [4], [8]-[10] has shown, these phase diagrams differ considerably for different s even though all values of s are in the same universality class for the usual paramagnetic (PM) to ferromagnetic (FM) phase transition in this model.

Another parameter of the Hamiltonian on which complex-temperature phase diagrams depend is the ratio of spin-spin couplings. Indeed, in cases such as the (spin 1/2, nearest-neighbor) Ising model on regular bipartite 2D lattices, where a variation in the ratio of spin-spin couplings along different lattice directions does not change the universality class of the PM to FM phase transition, this variation has a significant effect on the continuous locus of points where the free energy is non-analytic, which is denoted \mathcal{B} : while \mathcal{B} is a one-dimensional algebraic variety for the case of isotropic couplings, it becomes a two-dimensional variety for the non-isotropic case [14]. Recently, we have also shown, using exact results, that at complex-temperature singularities, the exponents describing the behavior of various thermodynamic functions depend, in general, on lattice type, which constitutes a violation of universality [5]. Moreover, we have found a number of violations of exponent relations at such singularities, such as $\gamma \neq \gamma'$ (for the susceptibility exponent) and $\alpha + 2\beta + \gamma \neq 2$ (as one approaches such a singularity from the PM phase) [5].

In the present paper, we explore further the extent of non-universal features of complex-temperature phase diagram of spin models, focussing on the effect of non-nearest-neighbor spin-spin couplings. Here, by “non-universal”, we mean features of the complex-temperature phase diagram that depend on a parameter in the Hamiltonian, where a variation of this parameter does not change the universality class of a phase transition at a given critical point. For our study, it will suffice to use a simple exactly solvable model, namely, the 1D Ising model with nearest-neighbor (NN) and next-to-nearest-neighbor (NNN) spin-spin couplings, J_{nn} and J_{nnn} . This model (except for the special case $J_{nnn} = -|J_{nn}|/2$) is critical at $T = 0$, so we specifically study the dependence of the complex-temperature phase diagram

on the ratio

$$r = \frac{J_{nnn}}{J_{nn}} \quad (1)$$

for the range of r values where changes in r do not change the ground state of the model or the universality class of the critical point at $T = 0$. After some early papers [15, 16], a detailed solution and discussion of this model was given by Stephenson in Ref. [17] and subsequent papers [18]. Some later papers include Refs. [19, 20]. All of these dealt with physical temperature; the model has not, to our knowledge, been studied for complex temperature. As our analysis of the complex-temperature phase diagram of this model will demonstrate, it illustrates very well how sensitive the CT phase diagram is to the presence of such NNN couplings. This example is also useful in giving one a qualitative idea, in a simple context, of what to expect concerning the effect of non-nearest-neighbor couplings in higher-dimensional spin models for which one does not have any exact solution. For these higher-dimensional models the addition of NNN couplings gives rise to quite complicated phase diagrams even for physical temperature [21]. Moreover, although $d = 1$ is the lower critical dimensionality for the Ising model, and some features, such as the lack of a physical phase transition at finite temperature are qualitatively different from the behavior in $d > d_\ell = 1$, past experience with $2 + \epsilon$ and $1 + \epsilon$ expansions [22] has shown that one can learn about spin models in intermediate dimensionalities by moving upward from d_ℓ as well as downward from the upper critical dimensionality d_u . Indeed, several intriguing connections were previously noted between the CT phase diagrams of the 1D spin s Ising model and features of the same model on the square lattice [8, 9]. In passing, it may be noted that the 1D NNN Ising model has also been used in a complementary manner in Ref. [23], for a study of Yang-Lee (complex-field) zeros of the partition function for physical temperature.

2 Ising Model and Notation

In this section, we shall briefly give the relevant notation and review some basic properties of the model for physical temperature which will serve as a background for our new results on the complex-temperature properties. The 1D (spin 1/2) Ising model with NN and NNN couplings is defined, for temperature T and external magnetic field H on a 1D lattice, by the partition function $Z = \sum_{\{\sigma_n\}} e^{-\beta\mathcal{H}}$ with Hamiltonian

$$\mathcal{H} = -J_{nn} \sum_n \sigma_n \sigma_{n+1} - J_{nnn} \sum_n \sigma_n \sigma_{n+2} - H \sum_n \sigma_n \quad (2)$$

where $\sigma_n = \pm 1$ and $\beta = (k_B T)^{-1}$. Except where otherwise indicated, we take $H = 0$ below. It is convenient to define

$$K = \beta J_{nn} \quad (3)$$

$$K' = \beta J_{nnn} \quad (4)$$

and $h = \beta H$. Recall that on a bipartite lattice Λ , without loss of generality, one may take $J_{nn} \geq 0$ (if $J_{nn} < 0$ initially, we can redefine $\sigma_n \rightarrow -\sigma_n$ for $n \in \Lambda_e$, $\sigma_n \rightarrow \sigma_n$ for $n \in \Lambda_o$, and $J_{nn} \rightarrow -J_{nn}$ where Λ_e and Λ_o denote the even and odd sublattices of Λ ; the partition function Z is invariant under this mapping). Using this fact, we shall thus take $J_{nn} > 0$ henceforth. We define the ratio of couplings by eq. (1). We shall mainly consider the effect of NNN couplings with $r \geq 0$ since (given that we take $J_{nn} > 0$), these NNN couplings do not introduce any frustration or competition and do not change the universality class or ground state of the model. In contrast, given that we take $J_{nn} > 0$, a NNN coupling with negative J_{nnn} does introduce such competition and frustration and is not necessarily an irrelevant perturbation to the Hamiltonian. We shall also include some results for negative J_{nnn} . It is convenient to define the Boltzmann weight variables $z = e^{-2K'}$,

$$u = z^2 = e^{-4K'} \quad (5)$$

and $z_K = e^{-2K}$, with

$$u_K = z_K^2 = e^{-4K} \quad (6)$$

For our study, it will be sufficient to consider the cases where (i) $r = 1/p$ where p is an integer, or (ii) r is an integer, since these already amply demonstrate the sensitivity of the complex-temperature phase diagram to the value of r . In these cases, Z is a generalized polynomial (i.e. with positive and negative integer powers) in the respective Boltzmann weights (i) u and (ii) u_K . Of course, one could also consider the case $r = p/q$ where $p \neq 1$ and $q \neq 1$ are relatively prime integers, but we shall not do this here. The (reduced, per site) free energy is defined as $f = -\beta F = \lim_{N \rightarrow \infty} N^{-1} \ln Z$ in the thermodynamic limit. We assume periodic boundary conditions and take the number of lattice sites N to be even in order to preserve the bipartite lattice structure on a finite lattice.

3 Generalities and Complex-Temperature Phases

For $d = 1$ dimension, it is straightforward to solve this model exactly, e.g., by transfer matrix methods. One has

$$Z = \text{Tr}(\mathcal{T}^N) = \sum_j \lambda_j^N \quad (7)$$

where the λ_j , $j = 1, \dots, 4$ denote the eigenvalues of the transfer matrix \mathcal{T} defined by $\mathcal{T}_{nn'} = \langle \ell_n | \exp(-\beta E(\ell_n, \ell_{n'})) | \ell_{n'} \rangle$. It is natural to analyze the phase diagram in complex plane of the appropriate Boltzmann weight variables (such as u or u_K for positive r). For physical

temperature, phase transitions are associated with degeneracy of leading eigenvalues. There is an obvious generalization of this to the case of complex temperature: in a given region of u or other Boltzmann weight variable, the eigenvalue of \mathcal{T} which has maximal magnitude, λ_{max} gives the dominant contribution to Z and hence, in the thermodynamic limit, f receives a contribution only from λ_{max} : $f = \ln(\lambda_{max})$. For complex K , f is, in general, also complex. The CT phase boundaries are determined by the degeneracy, in magnitude, of leading eigenvalues of \mathcal{T} . As one moves from a region with one dominant eigenvalue λ_{max} to a region in which a different eigenvalue λ'_{max} dominates, there is a non-analyticity in f as it switches from $f = \ln(\lambda_{max})$ to $f = \ln(\lambda'_{max})$. The boundaries of these regions are defined by the degeneracy condition among dominant eigenvalues, $|\lambda_{max}| = |\lambda'_{max}|$. These form curves in the plane of the given Boltzmann weight variable.

Of course, for physical temperature, a 1D spin model with finite-range interactions has no non-analyticities for any (finite) value of K , so that, in particular, the 1D NNN Ising model is analytic along the positive real axis in the complex u or u_K plane and is only singular at $T = 0$. In this context, we recall that the elements of the transfer matrix are non-negative (positive or zero) real functions of T for physical temperature, and the Perron-Frobenius theorem [24] guarantees that a (finite-dimensional, but not necessarily symmetric) square matrix with non-negative real entries has a real positive eigenvalue of greatest magnitude. This property underlies the absence of any non-analyticity and associated phase transition in a 1D spin model with finite-range interactions. However, when one generalizes the temperature to complex values, the elements of the transfer matrix are not, in general, non-negative (they are complex), so that the premise of the Perron-Frobenius theorem is no longer satisfied, and, indeed, the maximal eigenvalue can switch as one varies K over complex values.

Since the λ_j are analytic functions of u , whence $\lambda_j(u^*) = \lambda_j(u)^*$, it follows that the solutions to the degeneracy equations defining the boundaries between different phases, $|\lambda_i| = |\lambda_j|$, are invariant under $u \rightarrow u^*$. Hence the complex-temperature phase boundary \mathcal{B} , or equivalently, the continuous locus of points where the free energy f is non-analytic, is invariant under $u \rightarrow u^*$. The same applies for \mathcal{B} in the u_K plane, as discussed below. Although the model has a physical phase structure consisting only of the Z_2 -symmetric, disordered phase, its complex-temperature phase diagram is nontrivial and exhibits a number of interesting features.

Since the model has NNN couplings, one cannot define the transfer matrix as acting just between states consisting only of neighboring spins. The most compact way to define the transfer matrix is to use state vectors consisting of pairs of spins: $v_n = |\sigma_n, \sigma_{n+1}\rangle$. Then

$$\langle v_n | \mathcal{T} | v_{n+1} \rangle = \langle v_n | e^{-\beta \mathcal{H}} | v_{n+1} \rangle = \exp\left(\frac{K}{2}(\sigma_n \sigma_{n+1} + \sigma_{n+1} \sigma_{n+2}) + K' \sigma_n \sigma_{n+2} + h \sigma_{n+1}\right) \quad (8)$$

The factor of $(1/2)$ is included because each interaction of spins within a given vector $|v_n\rangle$ is counted twice in the sum over n . Hence, with the basis vectors ordered as $\{|v_n\rangle = |++\rangle, |+-\rangle, |-+\rangle, |--\rangle\}$, one has [15, 16]

$$\mathcal{T} = \begin{pmatrix} e^{K+K'+h} & e^{-K'+h} & 0 & 0 \\ 0 & 0 & e^{-K+K'-h} & e^{-K'-h} \\ e^{-K'+h} & e^{-K+K'+h} & 0 & 0 \\ 0 & 0 & e^{-K'-h} & e^{K+K'-h} \end{pmatrix} \quad (9)$$

Note that \mathcal{T} has zero matrix elements if the second spin in $|v_n\rangle$ has a value different from the first spin in $|v_{n+1}\rangle$, since these states overlap in this middle spin. Although \mathcal{T} is not symmetric, the usual relation $Z = \text{Tr}(\mathcal{T}^N) = \sum_j \lambda_j^N$, where the λ_j 's are the eigenvalues of \mathcal{T} , still holds; this follows from (i) the theorem [24] that an arbitrary complex $\ell \times \ell$ matrix can be put into upper triangular (u.t.) form by a unitary transformation V : $V\mathcal{T}V^{-1} = \mathcal{T}_{u.t.}$, such that $\text{diag}(\mathcal{T}_{u.t.}) = \{\lambda_1, \dots, \lambda_\ell\}$; and (ii) the identity $\text{Tr}(\mathcal{T}_{u.t.}^N) = \text{Tr}(\mathcal{T}^N) = \sum_{j=1}^\ell \lambda_j^N$. It is convenient to define $\bar{\mathcal{T}} = e^{-(K+K'+h)}\mathcal{T}$ so that $\bar{\mathcal{T}}_{11} = 1$ and consider the eigenvalues of $\bar{\mathcal{T}}$. We shall take $h = 0$ henceforth.

$\bar{\mathcal{T}}$ has the eigenvalues

$$\lambda_{1\pm} = e^{-K} \left[\cosh K \pm \sqrt{\sinh^2 K + e^{-4K'}} \right] \quad (10)$$

$$\lambda_{2\pm} = e^{-K} \left[\sinh K \pm \sqrt{\cosh^2 K - e^{-4K'}} \right] \quad (11)$$

For physical temperature, λ_{1+} is the dominant eigenvalue, so the (reduced, per site) free energy is $f = \ln(\lambda_{1+})$. In passing, we note that an equivalent method for solving the model in zero field is to re-express it formally in terms of a different theory with only NN couplings but a nonzero effective field [17].

The internal or configurational energy (per site) U is

$$U = -\frac{J_{nn} \sinh(K)}{\sqrt{\sinh^2(K) + e^{-4K'}}} - J_{nnn} \left[1 - \frac{2e^{-4K'}}{\sinh^2(K) + e^{-4K'} + \cosh(K) \sqrt{\sinh^2(K) + e^{-4K'}}} \right] \quad (12)$$

Observe that

$$U(J_{nn}, J_{nnn}, \beta) = U(-J_{nn}, J_{nnn}, \beta) \quad (13)$$

which is an explicit illustration of the general fact noted above that we can, without loss of generality, take $J_{nn} > 0$. The nature of the ground state (g.s.) depends on r [16]: if J_{nnn} is positive or sufficiently weakly negative, the ground state is ferromagnetic:

$$r > -\frac{1}{2} \implies \text{FM g.s.} \quad (14)$$

while for stronger negative J_{nnn} it changes according to

$$r < -\frac{1}{2} \implies (2, 2) \text{ g.s.} \quad (15)$$

where the $(2, 2)$ g.s. refers to a spin configuration of the modulated form $(++--++--\dots)$. Correspondingly, there is a non-analytic change in the ground state energy:

$$U(T=0) = -(J_{nn} + J_{nnn}) \quad \text{for } r \geq -\frac{1}{2} \quad (16)$$

whereas

$$U(T=0) = J_{nnn} \quad \text{for } r \leq -\frac{1}{2} \quad (17)$$

Evidently (given that we take $J_{nn} > 0$), negative values of J_{nnn} give rise to competing interactions and frustration. Indeed, if J_{nnn} is sufficiently negative that $r < -1/2$, it changes the ground state of the model. In our study of the dependence of the complex-temperature phase diagram on the addition of irrelevant operators (i.e., irrelevant in the sense that they do not change the $T=0$ critical behavior), we therefore shall restrict to the case $r > -1/2$. However, since the range $r \leq -1/2$ is of interest in its own right, we shall also briefly digress to discuss this case further below. As Stephenson showed [17, 18], even in the range $-1/2 < r < 0$, where the ground state still exhibits saturated FM long-range order, the NNN coupling has the interesting effect of giving rise to a “disorder temperature” T_D , where the correlation length has a local minimum; for $T < T_D$, the spin-spin correlation functions have a purely exponential asymptotic decay, while for $T > T_D$, their asymptotic decay is an exponential multiplied by an oscillatory factor.

The $T=0$ criticality of the model is typical of a theory at its lower critical dimensionality, here $d=1$. As $T \rightarrow 0$, the specific heat C has an essential zero given by

$$C \sim 4k_B(1+2r)^2 K^2 e^{-2(1+2r)K} \quad \text{as } T \rightarrow 0 \quad \text{for } r > -\frac{1}{2} \quad (18)$$

and

$$\begin{aligned} C &\sim \frac{k_B}{2}(1+2r)^2 K^2 e^{(1+2r)K} \\ &\sim \frac{k_B}{2}(1-2|r|)^2 K^2 e^{-(2|r|-1)K} \quad \text{as } T \rightarrow 0 \quad \text{for } r < -\frac{1}{2} \end{aligned} \quad (19)$$

while for the borderline value $r = -1/2$ one finds the proportionality

$$C \sim k_B A K^2 e^{-2K} \quad \text{for } r = -\frac{1}{2} \quad (20)$$

For $r \geq 0$ and for physical temperature, the spin-spin correlation function decays asymptotically like

$$\langle \sigma_0 \sigma_n \rangle \sim \left(\frac{\lambda_{2+}}{\lambda_{1+}} \right)^{|n|} \quad (21)$$

This is also true for $-1/2 < r < 0$ if $T < T_D$ [17, 18]. Hence, taking the $T \rightarrow 0$ limit, one finds that the correlation length ξ , defined as usual by $\xi^{-1} = -\lim_{n \rightarrow \infty} n^{-1} \ln |\langle \sigma_0 \sigma_n \rangle|$, diverges like

$$\xi \sim (1/2)e^{2(1+2r)K} \quad \text{as } T \rightarrow 0 \quad (22)$$

One also finds that for $r > -1/2$, the (zero-field) susceptibility χ diverges like

$$\chi \sim (1/2)\beta^{-1}e^{2(1+2r)K} \quad \text{as } T \rightarrow 0 \quad (23)$$

Consequently, for $r > -1/2$,

$$C \sim K^2 \xi^{-1}, \quad \chi \sim K^{-1} \xi \quad \text{as } T \rightarrow 0, \quad (24)$$

independent of r in this range. Thus, for $r > -1/2$, the singularities in C and χ , expressed as functions of the correlation length ξ , are independent of r in this range, which shows that for $r > -1/2$, the NNN coupling is an irrelevant perturbation, and the model satisfies weak universality in the sense of Suzuki [25], at the $T = 0$ critical point.

In order to investigate which eigenvalues are dominant in various complex-temperature phases, it is useful to express these as functions of the Boltzmann weight variables. For the case $r = 1/p$ with integral p , since Z is a generalized polynomial in u , the CT phase diagram is well defined in the complex u plane. This follows since the CT zeros of Z may be unambiguously calculated in the u plane, and, in the thermodynamic limit, these merge to form the phase boundary \mathcal{B} . In terms of the variable u ,

$$\lambda_{1\pm} = \frac{1}{2} \left[1 + u^{\frac{p}{2}} \pm \sqrt{(1 - u^{\frac{p}{2}})^2 + 4u^{1+\frac{p}{2}}} \right] \quad (25)$$

$$\lambda_{2\pm} = \frac{1}{2} \left[1 - u^{\frac{p}{2}} \pm \sqrt{(1 + u^{\frac{p}{2}})^2 - 4u^{1+\frac{p}{2}}} \right] \quad (26)$$

Note that

$$\lambda_{1\pm} \rightarrow \lambda_{2\pm} \quad \text{for } \sqrt{u} \rightarrow -\sqrt{u} \quad (27)$$

If p is an odd integer, then (27) implies that

$$\lambda_{1\pm}(u) = \lambda_{2\pm}(u^*) = \lambda_{2\pm}(u)^* \quad \text{for negative real } u \quad (28)$$

respectively for the \pm cases. (Here, we use the standard branch cut for \sqrt{u} , along the negative real u axis.)

As background, we recall that for the case of nearest-neighbor couplings, \mathcal{B} consists of the negative real axis in the u plane (e.g., Ref. [9]). This is evident from the fact that for $r = 0$, the two nontrivial eigenvalues of $\bar{\mathcal{T}}$ are $\lambda_{1+} = 1 + \sqrt{u}$ and $\lambda_{2+} = 1 - \sqrt{u}$, which are equal in magnitude for negative real u . (The other two eigenvalues, λ_{1-} and λ_{2-} both vanish.)

4 Case of $r = 1/p$ for Positive Integer p

We first consider the situation where the NNN coupling is of the same sign as, but weaker than, the NN coupling, i.e. $0 < r < 1$. For our purposes, it will suffice to deal with the case where $r = 1/p$ with p a positive integer. There are two subcases: p even and p odd. For even $p = 2\ell$, the eigenvalues of the transfer matrix have the following Taylor series expansions about $u = 0$:

$$\lambda_{1+} = 1 + u^{1+\frac{p}{2}} + \dots \quad (29)$$

$$\lambda_{2+} = 1 - u^{1+\frac{p}{2}} + \dots \quad (30)$$

$$\lambda_{1-} = u^{\frac{p}{2}} + \dots \quad (31)$$

$$\lambda_{2-} = -u^{\frac{p}{2}} + \dots \quad (32)$$

where \dots denote higher-order terms in u . It follows that for even p , λ_{1+} is the dominant eigenvalue on the positive real u axis and hence also in the complex-temperature phase which includes this axis. Furthermore, on the negative real u axis in the vicinity of the origin, (i) if $p = 0 \bmod 4$, i.e., ℓ is even, then λ_{2+} is the dominant eigenvalue, whereas (ii) if $p = 2 \bmod 4$, i.e., ℓ is odd, then λ_{1+} is the dominant eigenvalue; in both cases, the respective eigenvalues are therefore also dominant in the CT phases which include this portion of the negative real u axis near the origin. For odd positive integral p , the λ 's have analogous series expansions in the z plane, $\lambda_{1+} = 1 + z^{2+p} + \dots$, etc. Hence, in the u plane (with the usual $+$ sign taken for \sqrt{u} if $\arg(u) = 0$), λ_{1+} is again dominant on the positive real u axis in the vicinity of the origin.

Together with the theorem that a 1D spin model with finite-range interactions has no non-analyticity for $T > 0$, i.e., along the positive u axis, it follows that for positive integral p , λ_{1+} is the dominant eigenvalue on the entire positive u axis and hence the CT phase in the u plane which includes this axis and to which one can thus analytically continue from this axis.

We next prove a general theorem: For $r = 1/p$ with p a positive integer, there are $p + 2$ phase boundary curves emanating from the origin in the complex u plane, at the angles

$$\theta_n = \frac{(2n + 1)\pi}{2 + p}, \quad \text{for } n = 0, \dots, p + 1 \quad (33)$$

Proof: To encompass the cases of both even and odd p , we use the Taylor series expansions in the z plane. From these, it follows that in the vicinity of $z = 0$, λ_{1+} and λ_{2+} alternate as the dominant eigenvalues. Now define polar coordinates according to $z = \rho_z e^{i\theta_z}$, whence $u = \rho e^{i\theta}$ with $\rho = \rho_z^2$ and $\theta = 2\theta_z$; then the degeneracy condition of leading eigenvalues, $|\lambda_{1+}| = |\lambda_{2+}|$, reads $|1 + z^{2+p} + \dots| = |1 - z^{2+p} + \dots|$ (where \dots denote higher-order terms), the solution to which is $\cos((2 + p)\theta_z) = 0$, i.e., $\theta_z = (2n + 1)(\pi/2)/(2 + p)$ for $n = 0, \dots, p + 1$. This proves eq. (33).

A related theorem is: For positive, odd p , the complex-temperature phase boundary \mathcal{B} always contains the negative real u axis. To prove this, we again use the result that in the vicinity of $z = 0$, λ_{1+} and λ_{2+} alternate as the dominant eigenvalues. We next observe that in the u plane, the degeneracy condition of leading eigenvalues, $|\lambda_{1+}| = |\lambda_{2+}|$ is automatically satisfied on the negative real u axis as a consequence of the symmetry condition (27) and relation (28). This completes the proof.

Two further general theorems are the following: For positive $r = 1/p$ with integer p , as one makes a half-circuit around the origin in the u plane, the dominant eigenvalues alternate between λ_{1+} and λ_{2+} . This is proved by noting first that from the Taylor series expansions above, these two eigenvalues are the dominant ones in the vicinity of the origin, and second, it is precisely their alternation as dominant eigenvalues which produces the phase boundaries emanating from the origin at the angles (33) and separating the different phases. Since the dominant eigenvalue at $-\theta$ is the same as that at θ , this theorem also completely determines the dominant eigenvalues on the rest of the full circle around the origin.

By solving the degeneracy conditions of dominant eigenvalues, we have mapped out the complex-temperature phase diagrams. We consider odd values of p first and then even values. In Figs. 1-3 we show the results for $r = 1, 1/3$, and $1/5$.

For $r = 1$, we find that the complex-temperature phase diagram consists of three phases: (a) a region including the positive real u axis and extending outward to the circle at infinity, together with two complex-conjugate (c.c) phases (b), (b)*, located above and below the negative real u axis from the origin leftward to $u = -1$. As follows from our general discussion above, λ_{1+} is the dominant eigenvalue in region (a), and, since λ_{1+} and λ_{2+} alternate as dominant eigenvalues in the vicinity of $u = 0$, λ_{2+} is dominant in regions (b) and (b)*. On curve separating region (a) from regions (b) and (b)*, $|\lambda_{1+}| = |\lambda_{2+}|$. The CT phase boundary \mathcal{B} includes multiple points at $u = 0$, where three curves meet, and a multiple

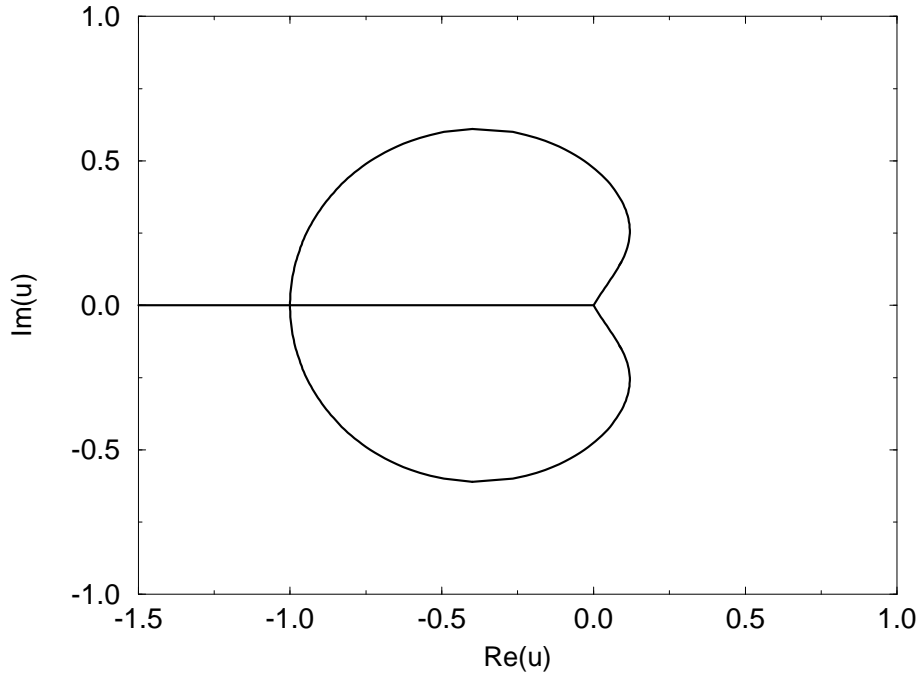


Figure 1: Phase diagram of the 1D NNN Ising model in the complex u plane for $J_{nnn}/J_{nn} = r = 1$.

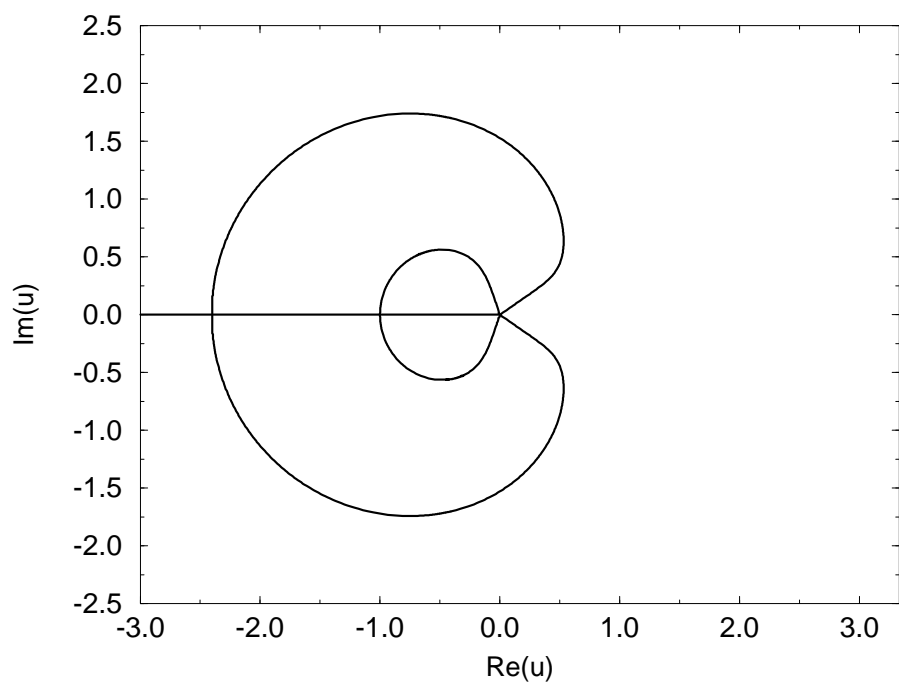


Figure 2: As in Fig. 1, for $r = 1/3$.

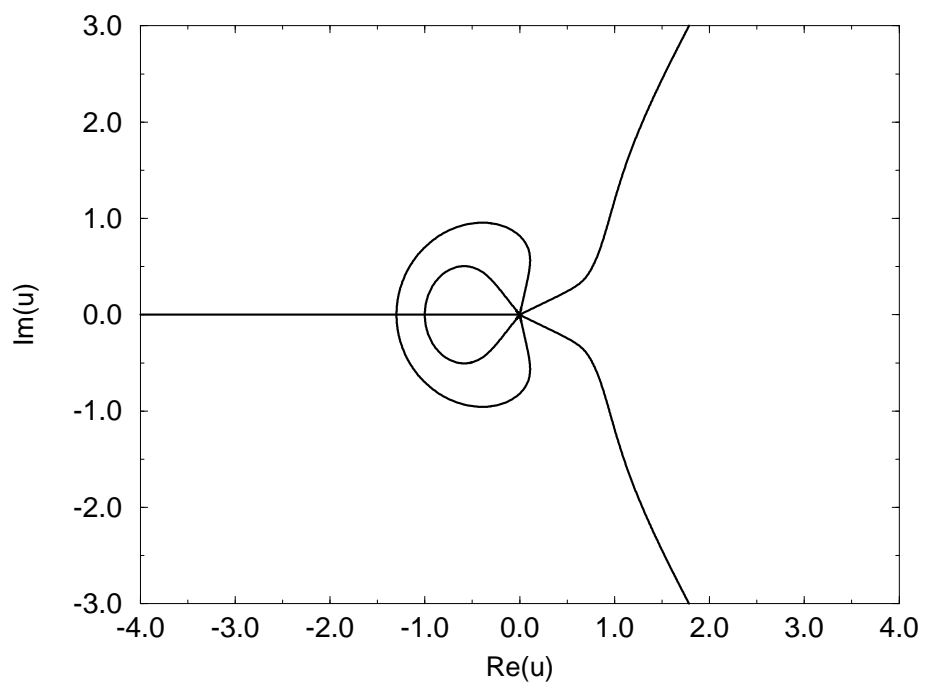


Figure 3: As in Fig. 1, for $r = 1/5$.

point at $u = -1$, where four curves meet, with 2 different tangents, hence index 2. Here, we use the term “multiple point” and “index” in their technical algebraic geometry sense (see our previous discussions in Ref. [6]). Thus, while in the model with only the NN spin-spin coupling, the CT phase boundary \mathcal{B} is the negative real axis, the effect of adding a NNN spin-spin coupling with $r = 1$ is to produce two new complex-conjugate phases bounded by curves starting out from the origin and meeting at $u = -1$. As must be true from general arguments, the theory is still analytic on the positive real u axis; the only changes are an increase in the number of CT phases elsewhere.

The complex-temperature phase diagram for $r = 1/3$, Fig. 2, is progressively more complicated, consisting of five phases: (a) a region containing the positive real u axis; (b), (b)*, complex-conjugate phases whose borders are shaped somewhat like half-circles, adjacent to the negative u axis and including the interval $-1 < u < 0$; and (c), (c)*, c.c. phases lying roughly concentrically outward from (b), (b)*, and including the interval of the negative real u axis $-2.4 \lesssim u < -1$. From our general discussion above, it follows that, in addition to region (a), λ_{1+} is dominant in regions (b) and (b)* while λ_{2+} is dominant in regions (c) and (c)*. The CT phase boundary \mathcal{B} contains multiple points at $u = 0$ where five curves come together, at $u = -1$ and $u \simeq -2.4$, where in each case four curves come together with two different tangents, hence index 2.

Finally, we show the complex-temperature phase diagram for $r = 1/5$ in Fig. 3. The general features of this phase diagram follow from our previous discussion. A new aspect is that in addition to the part of \mathcal{B} running along the negative real u axis, \mathcal{B} also contains two complex-conjugate curves which extend to infinite distance from the origin in the “northeast” and “southeast” quadrants.

We next show in Fig. 4 a typical CT phase diagram in the u plane for an even value, $p = 2$, i.e., $r = 1/2$. In contrast to the diagrams with odd p , in those with even p , \mathcal{B} does not contain the negative real axis. For $p = 2$, the CT phase diagram consists of four phases: (a) a region containing the positive real u axis and extending outwards to infinity; (b) a region including the interval $-1 < u < 0$; and complex conjugate regions (c), (c)* above and below region (b). Our general discussion above determines the dominant eigenvalues in the various regions: λ_{1+} in (a) and (b), and λ_{2+} in regions (c) and (c)*. The CT phase boundary \mathcal{B} involves multiple points at $u = 0$ and $u = -1$, each of index 2. The phase boundaries for even p may run to infinite distance from the origin. For example, we have also calculated the phase diagram for $p = 4$ case and find in this case that part of \mathcal{B} consists of curves running to $u = \pm i\infty$.

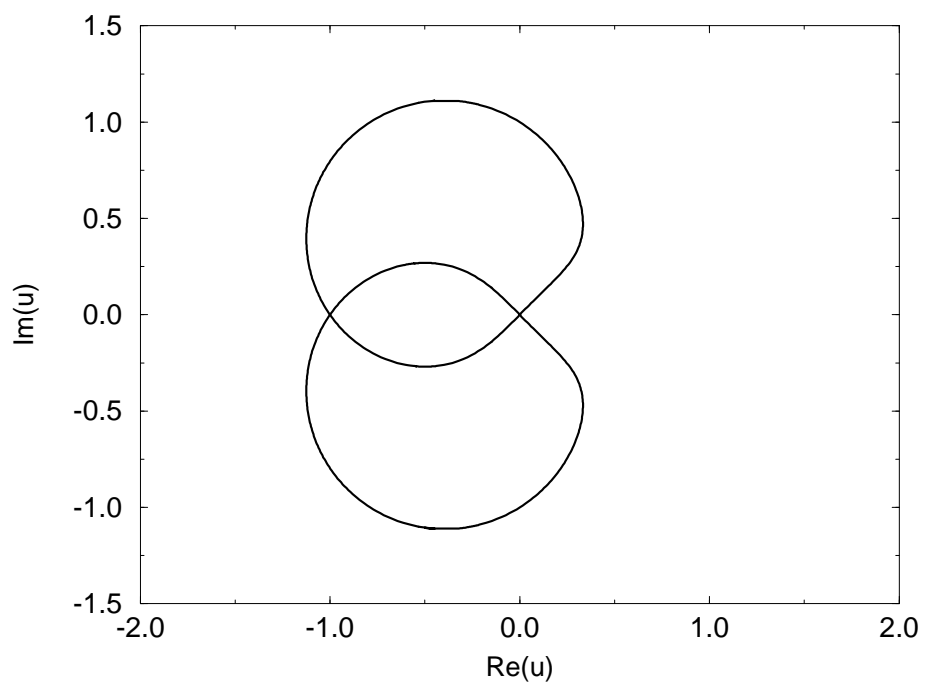


Figure 4: As in Fig. 1, for $r = 1/2$.

5 Case of Positive Integer r

We have also studied the situation where the NNN coupling is ferromagnetic and stronger than the NN coupling, i.e. $r \geq 1$; here, we focus on the case of positive integer r . For this case, the partition function is a generalized polynomial in u_K . By re-expressing the eigenvalues $\lambda_{1\pm}$ and $\lambda_{2\pm}$ as functions of u_K , i.e.,

$$\lambda_{1\pm} = \frac{1}{2} \left[1 + u_K^{\frac{1}{2}} \pm \sqrt{(1 - u_K^{\frac{1}{2}})^2 + 4u_K^{\frac{1}{2}+r}} \right] \quad (34)$$

$$\lambda_{2\pm} = \frac{1}{2} \left[1 - u_K^{\frac{1}{2}} \pm \sqrt{(1 + u_K^{\frac{1}{2}})^2 - 4u_K^{\frac{1}{2}+r}} \right] \quad (35)$$

one sees that

$$|\lambda_{1+}(u_K)| = |\lambda_{2+}(u_K)|, \quad |\lambda_{1-}(u_K)| = |\lambda_{2-}(u_K)| \quad \text{for real } u_K < 0 \quad (36)$$

This implies that the CT phase boundary \mathcal{B} contains the negative real u_K . The expansions of these four eigenvalues around the origin of the u_K plane follow directly from the expansions given in eqs. (29)-(32) with the replacement $u = u_K^r$. Hence, it is again true that as one traverses a half-circuit of the origin in the u_K plane, the dominant eigenvalue along the positive real u_K axis is λ_{1+} and the dominant eigenvalues alternate between λ_{1+} and λ_{2+} . This also determines the dominant eigenvalues on the complex-conjugate half-circuit. These two results together imply that for arbitrary positive integral p , the CT phase boundary \mathcal{B} always includes the negative real u_K axis.

Re-expressing the Taylor series expansions of the eigenvalues in terms of z_K , the degeneracy condition for the leading eigenvalues, $|\lambda_{1+}| = |\lambda_{2+}|$ reads $|1 + z_K^{1+2r} + \dots| = |1 - z_K^{1+2r} + \dots|$, where \dots denote higher-order terms. Denoting $u_K = \rho_K e^{i\theta_K}$, the solution to this condition is

$$\theta_K = \frac{(2n+1)\pi}{1+2r} \quad \text{for } n = 0, \dots, 2r \quad (37)$$

This proves that in the complex-temperature phase diagram in the u_K plane, \mathcal{B} contains $1 + 2r$ curves emanating from the origin at the angles given in eq. (37).

In Fig. 5 we show the complex-temperature phase diagram for a typical case, $r = 2$. The dominant eigenvalues in the phases which are contiguous to the origin $u_K = 0$ are completely determined by our previous general results; starting from the phase containing the positive real u_K axis and moving in the direction of increasing $\arg(u_K)$, these alternate according to λ_{1+} , λ_{2+} , and λ_{1+} . For the remaining phase which is not contiguous to the origin, depending on one's choices of branch cuts connecting the branch points of the square roots in the eigenvalues, either λ_{2+} or λ_{2-} is dominant.

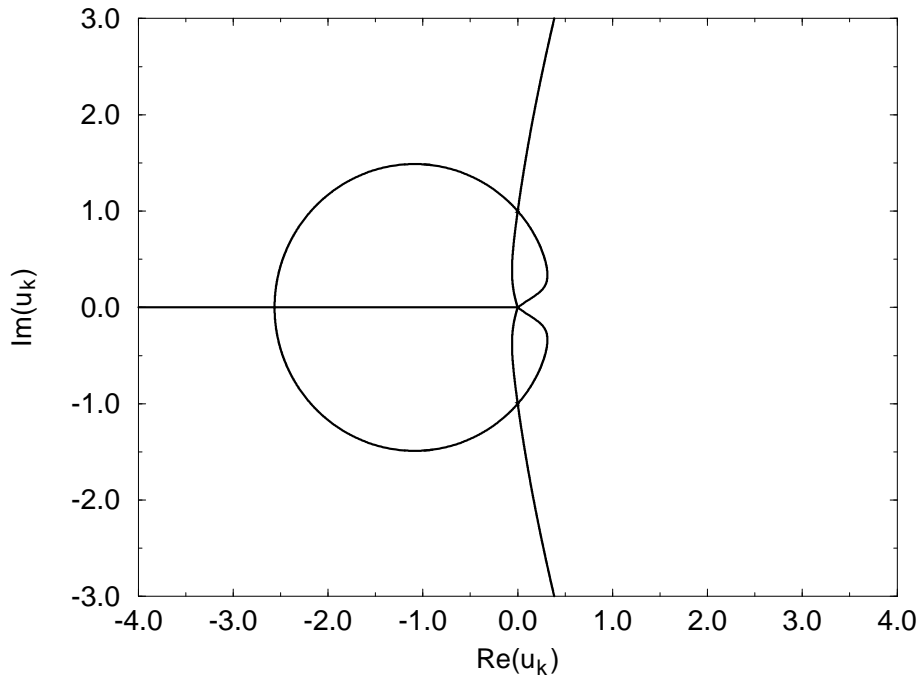


Figure 5: Complex-temperature phase diagram in the u_K plane for $r = 2$.

6 Negative r in the Interval $-1/2 < r < 0$

For the range $-1/2 < r < 0$, notwithstanding the competition and frustration which the NNN interaction produces, it is still an irrelevant perturbation. As before, if $1/r = -p$ with positive integral p , then Z is a generalized polynomial in the variable $u = e^{-4K'}$ and hence also in its inverse, $w = 1/u$. Since $K' < 0$, we shall use this inverse variable w for our analysis, in order to maintain the correspondence of zero temperature with the origin of the plots. The eigenvalues of the transfer matrix $\bar{\mathcal{T}}$ in this variable can be obtained from eqs. (25) and (26):

$$\lambda_{1\pm} = \frac{1}{2} \left[1 + w^{\frac{p}{2}} \pm \sqrt{(1 - w^{\frac{p}{2}})^2 + 4w^{\frac{p}{2}-1}} \right] \quad (38)$$

$$\lambda_{2\pm} = \frac{1}{2} \left[1 - w^{\frac{p}{2}} \pm \sqrt{(1 + w^{\frac{p}{2}})^2 - 4w^{\frac{p}{2}-1}} \right] \quad (39)$$

The borderline value $p = 2$, i.e., $r = -1/2$ at which the nature of the ground state changes, as discussed above, is evident in these eigenvalues since as p increases above $p = 2$, i.e., r decreases below $r = -1/2$, the eigenvalues cease to be finite at the origin $w = 0$ because the last term in the square root becomes a negative power. By the same reasoning as before, if and only if p is an odd integer, \mathcal{B} contains the negative real w axis. For integer $p > 2$, so that $r > -1/2$, which includes the region of interest here, these eigenvalues have the series expansions around $w = 0$

$$\lambda_{1+} = 1 + w^{\frac{p}{2}-1} + \dots \quad (40)$$

$$\lambda_{2+} = 1 - w^{\frac{p}{2}-1} + \dots \quad (41)$$

$$\lambda_{1-} = -w^{\frac{p}{2}-1} + \dots \quad (42)$$

$$\lambda_{1+} = w^{\frac{p}{2}-1} + \dots \quad (43)$$

where \dots denote higher order terms. From this it follows that for our case of integer $p > 2$, λ_{1+} is the dominant eigenvalue on the positive real w axis and in the CT phase which includes this axis. Other results are similar to those derived for positive $r = 1/p$ above: on the negative real w axis in the vicinity of the origin, if p is even, then (i) if $p = 0 \bmod 4$, then λ_{2+} is the dominant eigenvalue, whereas (ii) if $p = 2 \bmod 4$, then λ_{1+} is dominant, and these respective eigenvalues are also dominant in the CT phase which includes this portion of the negative real w axis.

In Fig. 6 and 7 we show our calculation of the complex-temperature phase diagram in the w plane for the values $r = -1/4$ and $r = -1/3$, respectively. For $r = -1/4$, besides (a) the wedge-shaped phase including the positive real w axis, where λ_{1+} is dominant, there is a phase (b) which includes the interval $-1 < w < 0$ of the w axis, in which λ_{2+} dominates, and

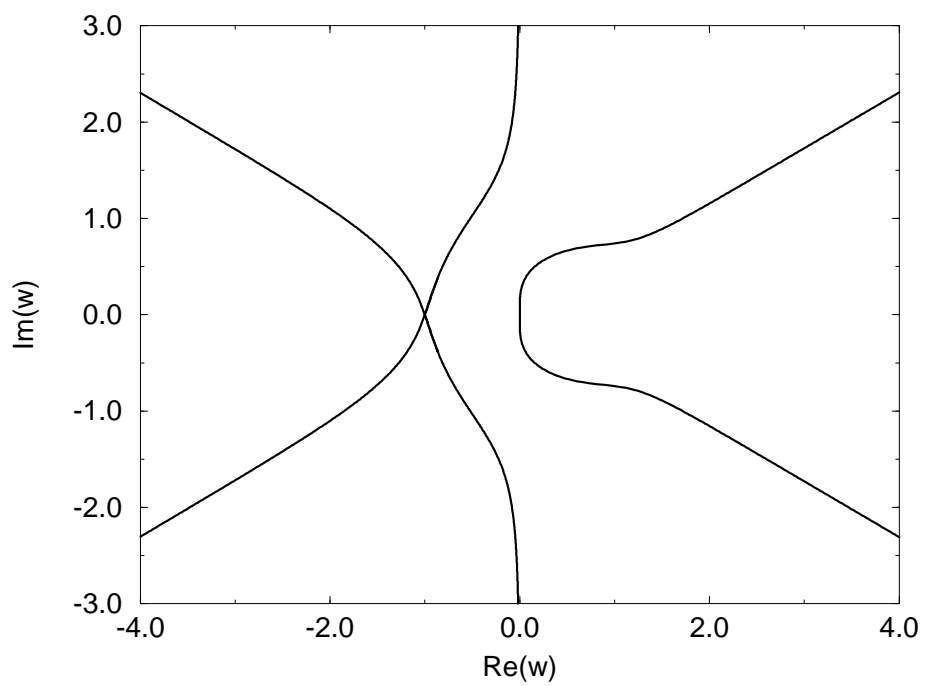


Figure 6: Complex-temperature phase diagram in the w plane for $r = -1/4$.

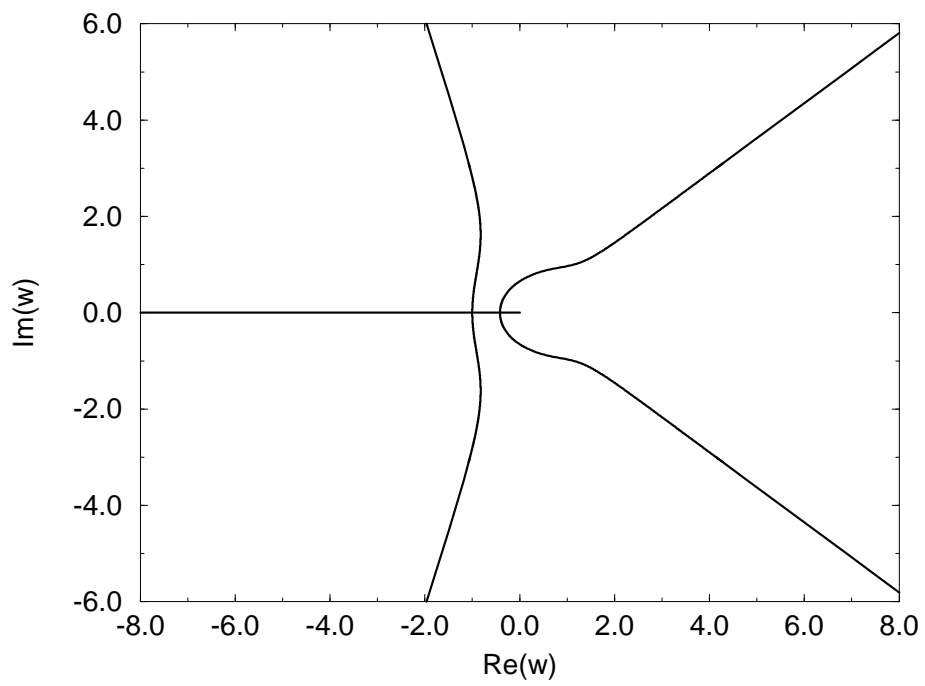


Figure 7: Complex-temperature phase diagram in the w plane for $r = -1/3$.

(c) a phase including the segment $-\infty < w < -1$ where λ_{2-} is dominant. In addition, there are two complex-conjugate phases (d) and (d)* where λ_{1-} is dominant; these have boundaries which cross each other at a multiple point of index 2 at $w = -1$. For $r = -1/3$, besides the phase containing the positive real w axis, there are two pairs of complex-conjugate phases. As one moves from northeast to northwest, the eigenvalues which are dominant in these regions are λ_{2+} and λ_{1-} .

For the present range $-1/2 < r < 0$, there is a finite physical disorder temperature T_D determined by the equation [17, 18]

$$\cosh(K) = e^{-2K'} \quad (44)$$

The disorder temperature T_D decreases monotonically from $T_D = \infty$ at $r = 0$ to $T_D = 0$ as r decreases to $-1/2$. In the context of the complex-temperature generalization of this model, we observe that, in addition to the physical solution of (44) for T_D , there are also complex-temperature solutions. In terms of the ratio r and the coupling $K = K_R + iK_I$, the real and imaginary parts of eq. (44) yield the respective equations

$$\cosh(K_R) \cos(K_I) = e^{-2rK_R} \cos(2rK_I) \quad (45)$$

$$\sinh(K_R) \sin(K_I) = -e^{-2rK_R} \sin(2rK_I) \quad (46)$$

A more compact way of writing (44) is in terms of the Boltzmann variable z_K :

$$1 + z_K = 2z_K^{r+\frac{1}{2}} \quad (47)$$

Let us define $K_D = J_{nn}/(k_B T_D)$ and $z_K = e^{-2K_D}$. As an illustration, for $r = -1/4$, eq. (47), expressed in terms of the variable $\omega = w^{1/2}$, where $w = e^{4K'}$ (whence, $w(r = -1/4) = z_K^{1/2} = e^{-K}$) is $(\omega - 1)(\omega^3 + \omega^2 + \omega - 1) = 0$. (The trivial solution $\omega = 1$ corresponds to $K = K' = 0$ in (44) and is not of interest here.) The cubic factor has as roots the physical disorder solution $\omega_D = 0.5437$, i.e., $w_D = 0.2956$ ($K_D = 1.219$) and, in addition, the complex-temperature roots $\omega = -0.7718 \pm 1.115i$, i.e., $w = -0.6478 \pm 1.721i$ ($K = -0.6094 \pm 1.931i$). As noted in Ref. [2], there are an infinite number of complex K values corresponding to a given value of a Boltzmann weight variable, depending on one's choice of Riemann sheet in the evaluation of the logarithm; here, we list only one value of K for each w . These complex-temperature solutions of (44) lie in the phases (d) and (d)* in Fig. 6. From a similar analysis for $r = -1/3$, where $w(r = -1/3) = e^{-4K/3}$, we find, besides the physical disorder point $w_D = 0.06694$ ($K_D = 2.028$), also the two pairs of complex-temperature solutions $w = -1.607 \pm 1.539i$ ($K = -0.5998 \pm 1.783i$) and $w = 1.073 \pm 1.366i$ ($K = -0.4142 \pm 0.6787i$). One can see from Fig. 7 that these complex-temperature solutions of (44) lie in the interiors of four CT phases.

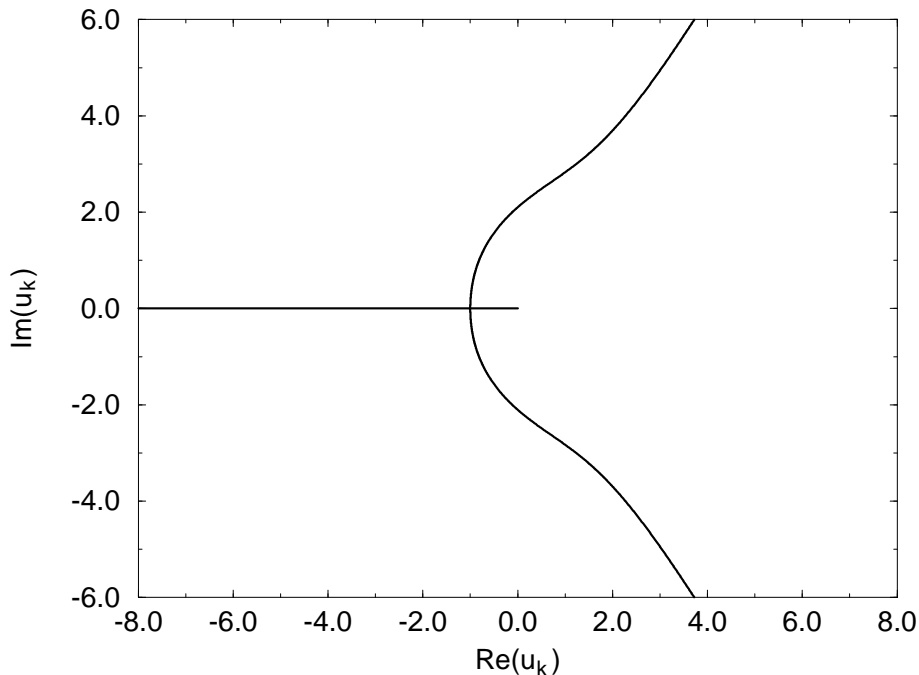


Figure 8: Complex-temperature phase diagram in the u_K plane for $r = -1$.

7 Negative r in the Interval $-\infty < r < -1/2$

As discussed above, for $r \leq -1/2$, the NNN spin-spin coupling is so strong as to change the nature of the ground state from FM to the (2,2) form. In Fig. 8 we show the complex-temperature phase diagram for a typical case, $r = -1$. Note that, in particular, by the same reasoning as for positive integer r (c.f. eq. (36)), it follows that \mathcal{B} always includes the negative real u_K axis.

8 Case $r = -1/2$

For the borderline value $r = -1/2$, i.e., $J_{nnn} = -(1/2)J_{nn} < 0$, the competing preferences toward a ferromagnetic and (2,2) ground state are exactly balanced. Indeed, for $r = -1/2$, the model has nonzero ground state entropy, $S(T=0) = k_B \ln\{(1/2)(1+\sqrt{5})\}$ [17, 20], and

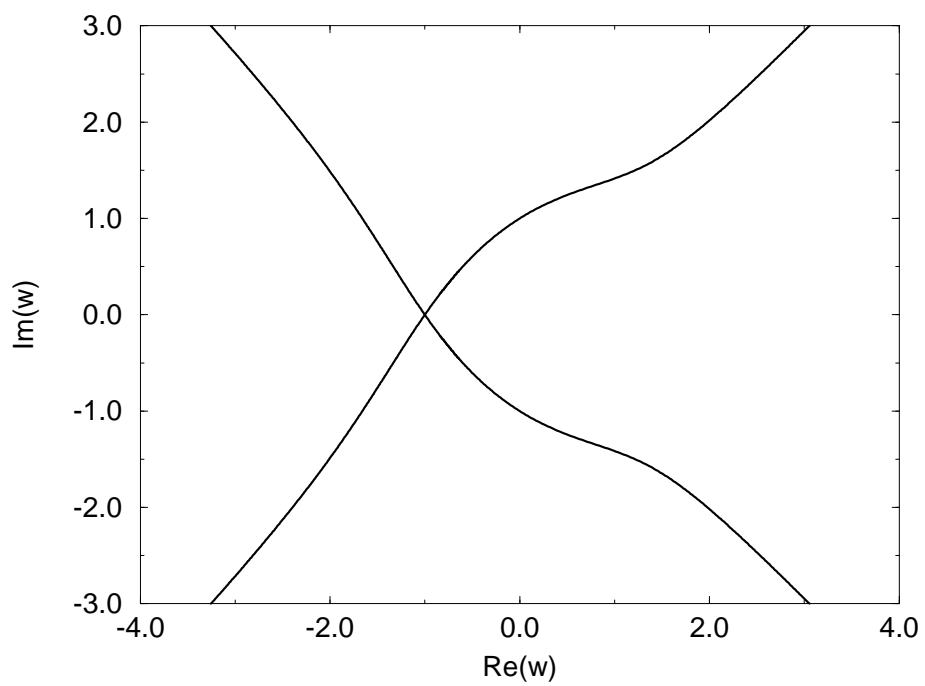


Figure 9: Complex-temperature phase diagram in the w plane, for $r = -1/2$.

exponential asymptotic decay of $\langle \sigma_0 \sigma_n \rangle$ (modulated by an oscillatory factor) even at $T = 0$ [17, 18]. We find that if and only if $r = -1/2$, then the complex-temperature phase boundary \mathcal{B} does not pass through the point $T = 0$, or equivalently, the origin in the $w = 1/u = e^{4K'}$ plane. This avoidance of the point $w = 0$ by \mathcal{B} shows the absence of criticality at $T = 0$. In Fig. 9 we present our calculation of the complex-temperature phase diagram for $r = -1/2$. One sees that \mathcal{B} consists of two complex-conjugate curves which only intersect the real w axis at the point $w = -1$ (where they exhibit a multiple point of index 2).

9 Potts Model

Since the spin 1/2 Ising model is equivalent to the two-state Potts model, it is natural to extend the present study to include some remarks on how the complex-temperature phase diagram of the 1D Potts model changes under the addition of a NNN coupling which is an irrelevant operator. Recall that in contrast to the 2D NN (spin 1/2) Ising model, no exact solution is known for general temperature of the 2D NN q state Potts model for $q > 2$ and hence the CT boundary \mathcal{B} is not known even for this NN case (see, e.g., Refs. [12, 13] and references therein).

The zero-field 1D q -state Potts model with NN and NNN interactions is defined by the partition function $Z_P = \sum_{\sigma_n} e^{-\beta \mathcal{H}_P}$ with

$$\mathcal{H}_P = -J_{nn} \sum_n \delta_{\sigma_n \sigma_{n+1}} - J_{nnn} \sum_n \delta_{\sigma_n \sigma_{n+2}} \quad (48)$$

where δ_{ij} is the Kronecker delta and $\sigma_n \in \{1, \dots, q\}$. For our study, we shall consider ferromagnetic couplings, $J_{nn}, J_{nnn} > 0$ and define K, K', r as in eqs. (3)-(1), and $u_P = e^{-K}$. The 1D NN model with $J_{nn} < 0$ involves finite ground state disorder, with ground state entropy $S_0 = k_B \ln(q-1)$. This is similar to the situation on several higher-dimensional lattices; see Ref. [26] for the square lattice and Ref. [27] for the honeycomb lattice.

A notable feature of the CT phase diagram for the 1D NN Potts model is its simplicity; in Ref. [9] we found that for $q \geq 3$, it consists only of two phases, separated by the boundary \mathcal{B} comprised of a circle

$$u_P = \frac{-1 + e^{i\omega}}{q-2}, \quad 0 \leq \omega < 2\pi \quad (49)$$

The solution of the 1D NNN Potts model proceeds in the standard manner, via transfer matrix methods. As before, it is most efficient to use spin configuration vectors $v_n = |\sigma_n, \sigma_{n+1}\rangle$, so that

$$\langle v_n | \mathcal{T}_P | v_{n+1} \rangle = \langle v_n | e^{-\beta \mathcal{H}} | v_{n+1} \rangle = \exp\left(\frac{K}{2}(\delta_{\sigma_n \sigma_{n+1}} + \delta_{\sigma_{n+1} \sigma_{n+2}}) + K' \delta_{\sigma_n \sigma_{n+2}}\right) \quad (50)$$

Thus the transfer matrix \mathcal{T}_P is a $q^2 \times q^2$ matrix. Here we consider the simplest case, $q = 3$. The resultant \mathcal{T}_P is straightforwardly calculated from (50). Defining $\bar{\mathcal{T}}_P = e^{-(K+K'+h)}\mathcal{T}_P$, we find for the characteristic polynomial of $\bar{\mathcal{T}}_P$:

$$P(\bar{\mathcal{T}}_P; \lambda) = \left(\lambda + u_P(1 - u_P) \right) \left(\lambda^2 - (u_P^2 + u_P + 1)\lambda + u_P(1 - u_P)(1 + 2u_P) \right) \times \\ \times \left(\lambda^3 + (u_P^2 - 1)\lambda^2 + u_P^2(u_P - 1)(u_P + 2)\lambda + u_P^2(1 - u_P)^2(2u_P + 1) \right)^2 \quad (51)$$

The resultant eigenvalues of $\bar{\mathcal{T}}_P$ are

$$\lambda_0 = u_P(u_P - 1) \quad (52)$$

$$\lambda_{1\pm} = \frac{1}{2} \left[1 + u_P + u_P^2 \pm \sqrt{1 - 2u_P - u_P^2 + 10u_P^3 + u_P^4} \right] \quad (53)$$

together with three roots of the cubic factor in (51), each of which is a double root of $P(\bar{\mathcal{T}}_P; \lambda)$. We denote these as λ_{3a} , λ_{3b} , and λ_{3c} and, since the expressions for these cubic roots are rather complicated, we omit listing them here. Aside from the polynomial λ_0 , the other eigenvalues have the following Taylor series expansions around $u_P = 0$:

$$\lambda_{1+} = 1 + 2u_P^3 + O(u_P^4) \quad (54)$$

$$\lambda_{1-} = u_P + u_P^2 + O(u_P^3) \quad (55)$$

$$\lambda_{3a} = 1 - u_P^3 + O(u_P^4) \quad (56)$$

$$\lambda_{3b} = -u_P - \frac{1}{2}u_P^2 + O(u_P^3) \quad (57)$$

$$\lambda_{3c} = u_P - \frac{1}{2}u_P^2 + O(u_P^3) \quad (58)$$

In the absence of any NNN coupling, eq. (49) shows that \mathcal{B} would be a circle of radius 1 centered at $u_P = -1$. In Fig. 10 we show the complex-temperature phase diagram for $r = 1$. We find that the presence of the NNN interaction has a strong effect on this diagram. The CT phase boundary is much more complicated than just the unit circle centered at $u_P = -1$. Rather than just two regions, as in the model with only NN spin-spin interactions, the complex-temperature phase diagram consists of nine phases. Three of these are (a) the region containing the positive real u_P axis, where λ_{1+} is dominant; (b) the region including the interval $-1 < u_P < 0$, in which λ_{3a} is dominant; and (c) the region including the rest of the negative real axis, $-\infty < u_P < -1$, where λ_0 is dominant. The remaining six are comprised of three complex conjugate pairs. Starting from the northeast quadrant and moving to the northwest quadrant, the members of these pairs with $Im(u_P) > 0$ are (d) a region with a wedge contiguous to the origin, where λ_{3a} is dominant; (e) a second region

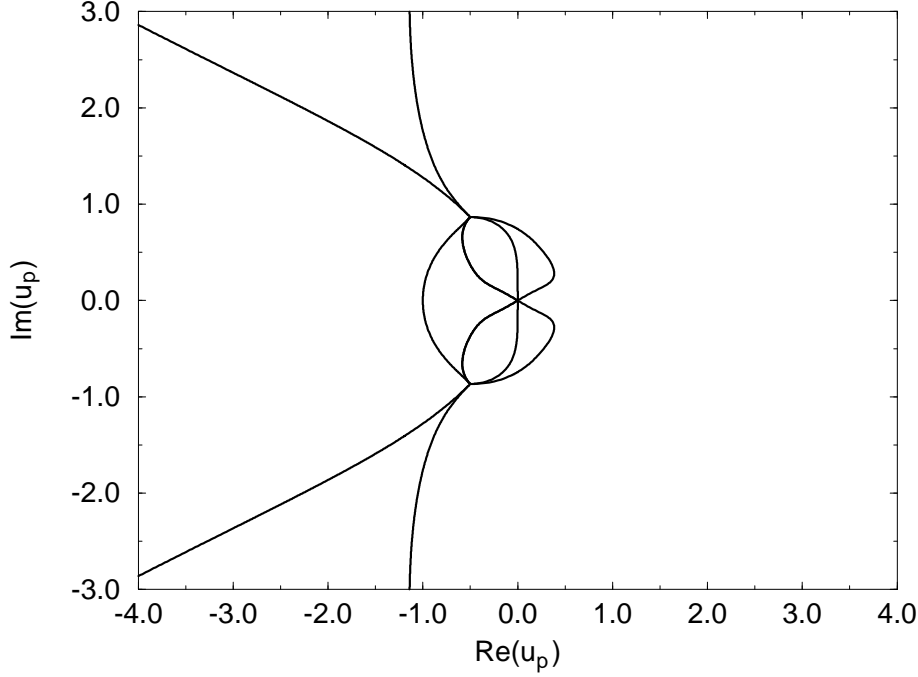


Figure 10: Complex-temperature phase diagram of the 1D $q = 3$ Potts model in the u_P plane for $r = 1$.

contiguous to the origin, where λ_{1+} is dominant, and (f) at the same angle, $\simeq 2\pi/3$, but farther out from the origin, a region where, depending on how the cuts linking the branch points of the cube roots are chosen, λ_{3b} or λ_{3c} is dominant; the others are then the complex conjugates of these. The complex-temperature boundary \mathcal{B} contains a multiple point at $u_P = 0$, where six curves come together with three separate tangents (hence index 3), and two complex conjugate multiple points at $(u_P)_m = e^{2\pi i/3}$ and $(u_P)_m^*$, where six curves meet in a tacnode, with three different tangents (see Ref. [6] for a discussion of tacnodes on CT boundaries \mathcal{B}). We note that the complex conjugate boundary curves separating phases (a) and (f) and (a) and (f)*, respectively, eventually head outward in northeast and southeast directions at larger distance $|u_P|$ from the origin.

10 Conclusions

In this work we have continued our exploration of the dependence of complex-temperature phase diagrams on details of the Hamiltonian, focussing on the effect of a next-nearest-neighbor spin-spin coupling in a simple exactly solvable model, the 1D Ising model with nearest- and next-nearest-neighbor spin-spin couplings. Even for the range of values of $r = J_{nnn}/J_{nn}$ where the NNN coupling is an irrelevant perturbation to the Hamiltonian at the $T = 0$ critical point, we have shown that it has a considerable effect on the complex-temperature phase diagram. We have also presented some corresponding findings for the 1D $q = 3$ Potts model. Our results further emphasize that, while complex-temperature phase diagrams and singularities give a deeper insight into the behavior of statistical mechanical models, they depend on details of the Hamiltonian, in contrast to the usual universality observed at physical critical points.

This research was supported in part by the NSF grant PHY-93-09888.

References

- [1] C. N. Yang and T. D. Lee, Phys. Rev. **87**, 404 (1952); T. D. Lee and C. N. Yang, *ibid.* **87**, 410 (1952).
- [2] G. Marchesini and R. Shrock, Nucl. Phys. B **318**, 541 (1989).
- [3] R. Abe, T. Dotera, and T. Ogawa, Prog. Theor. Phys. **85**, 509 (1991).
- [4] I. G. Enting, A. J. Guttmann, and I. Jensen, J. Phys. A **27**, 6963 (1994).
- [5] V. Matveev and R. Shrock, J. Phys. A **28**, 1557 (1995); *ibid.*, **29**, 803 (1996).
- [6] V. Matveev and R. Shrock, J. Phys. A **28**, 5235 (1995).
- [7] V. Matveev and R. Shrock, J. Phys. A **28**, 4859 (1995); Phys. Rev. **E53**, 254 (1996).
- [8] V. Matveev and R. Shrock, J. Phys. A (Lett.) **28**, L533 (1995).
- [9] V. Matveev and R. Shrock Phys. Lett. **A204**, 353 (1995).
- [10] I. Jensen, A. J. Guttmann, and I. G. Enting, J. Phys. A **29**, 3805 (1996).
- [11] P. P. Martin, *Potts Models and Related Problems in Statistical Mechanics* (World Scientific, Singapore, 1991).

- [12] C. N. Chen, C. K. Hu, and F. Y. Wu, Phys. Rev. Lett. **76**, 169 (1996); F. Y. Wu, G. Rollet, H. Y. Huang, J. M. Maillard, C. K. Hu, and C. N. Chen, *ibid.* **76**, 173 (1996).
- [13] V. Matveev and R. Shrock, Phys. Rev. **E54**, 6174 (1996) (cond-mat/9605176).
- [14] W. van Saarloos, and D. Kurtze, J. Phys. A **17**, 1301 (1984); J. Stephenson and R. Couzens, Physica **129A**, 201 (1984); D. Wood, J. Phys. A **18**, L481 (1985); J. Stephenson, Physica **136A**, 147 (1986); J. Stephenson and J. van Aalst, *ibid.* **136A**, 160 (1986); J. Stephenson, *ibid.* **148A**, 88, 107 (1988).
- [15] E. Montroll, J. Chem. Phys. **10**, 61 (1941).
- [16] T. Oguchi, J. Phys. Soc. Jpn. **20**, 2236 (1965).
- [17] J. Stephenson, Can. J. Phys. **48**, 1724 (1970).
- [18] J. Stephenson, Can. J. Phys. **48**, 2118 (1970); Phys. Rev. **B1**, 4405 (1970); J. Stephenson and D. D. Betts, Phys. Rev. **B2**, 2702 (1970); J. Stephenson, Phys. Rev. **B15**, 5442, 5453 (1977).
- [19] R. M. Hornreich, R. Leibmann, H. G. Schuster, and W. Selke, Zeit. f. Phys. **B35**, 91 (1979).
- [20] S. Redner, J. Stat. Phys. **25**, 15 (1981).
- [21] W. Selke, Phys. Rept. **170**, 213 (1988).
- [22] A. A. Migdal, Zh. Eksp. Teor. Fiz. **69**, 1457 (1975) (JETP **42**, 743 (1975)); A. M. Polyakov, Phys. Lett. **B59**, 79 (1975); E. Brézin and J. Zinn-Justin, Phys. Rev. Lett. **36**, 691 (1976); Phys. Rev. **B14**, 3110 (1976); W. Bardeen, B. W. Lee, and R. Shrock, Phys. Rev. **D14**, 985 (1976).
- [23] S. Katsura and M. Ohminami, J. Phys. A **5**, 95 (1972).
- [24] R. Bellman, *Introduction to Matrix Analysis* (McGraw-Hill, New York, 1960).
- [25] M. Suzuki, Prog. Theor. Phys. **51**, 1992 (1974).
- [26] R. J. Baxter, Proc. Roy. Soc. London, Ser. A **383**, 43 (1982).
- [27] R. Shrock and S.-H. Tsai, J. Phys. A **30**, 495 (1997) (cond-mat/9608095).